Comparison of Electrochemically and Photochemically Induced Electron-Transfer Processes of a Series of Copper(II) Schiff Base Complexes with Thiolate Coordination

Stephan Knoblauch,[a] František Hartl,*[b] Derk J. Stufkens,[b] and Horst Hennig*[a]

Dedicated to Professor Arnd Vogler on the occasion of his 60th birthday

Keywords: Spectroelectrochemistry / Cyclic voltammetry / Photochemistry / Copper(II) complexes / Thiolate complexes

The electrochemical and photoredox properties of copper(II) thiopyrazolone Schiff base complexes **1**–**9** with imine and thiolate coordination, showing variable degrees of tetrahedral distortion, were investigated by means of combined electrochemical and spectroscopic techniques in the temperature range of 193−293 K. The cyclic voltammograms of **1**–**9** in butyronitrile revealed that the reduction and oxidation paths are strongly dependent on the geometry of the CuN_2S_2 moiety. Due to the strong delocalization of the singly occupied redox orbital (SOMO) the oxidations and reductions occur in a narrow potential range. The one-electron-reduced **1(r)**–**9(r)** and oxidized **1(o)**–**9(o)** products were electrogenerated and stabilized inside optically transparent thin-layer electrochemical (OTTLE) cells at variable temperatures and could be characterized for the first time by UV/Vis spectroscopy. The reduced formal d^{10} copper(I) species absorb only weakly in the visible region. The oxidized products **1(o)**–**9(o)** show several strong absorptions in the visible region due to the presence of formal d^8 copper(III) species. The spectral information allowed assignment of the initial photoproducts. Irradiations in donor media such as THF or EtOH initially produces **1(r)**–**9(r)**. No photoreduction was observed in *t*BuOH which cannot liberate reducing H_α. The primary oxidized species **1(o)**–**9(o)** were formed in chlorinated acceptor solvents ($CHCl_3$) on UV irradation. Fast relaxation to the ground state prevents the photoredox reactions from CT or LF excited states.

Introduction

Recently we have shown that the photocatalytic oxygenation of terpenes like α-pinene induced by iron(III) porphyrins leads in the presence of copper(II) complexes with $[CuN_2S_2]$ constitution to rearrangement of α-pinene to limonene (beside the formation of oxygenation products).[1] $[CuN_2S_2]$ complexes containing Schiff base ligands with imine and thiolate coordination sites (Figure 1) are of particular significance in that photocatalytic rearrangement. Because it is assumed that photoinduced electron-transfer processes between iron(III) porphyrins, $[CuN_2S_2]$ complexes and α-pinene occur, the spectroscopic, electrochemical, and photochemical properties of the copper(II) complexes themselves were investigated to obtain more insight into the rather intricate function of these complexes. This paper summarizes results obtained from combined electrochemical and photochemical investigations of copper(II) complexes of Schiff base ligands with imine and thiolate coordination sites.

The well-known procedure of the synthesis of these ligands by condensation of the 4-benzoyl-5-mercapto-3-methyl-1-phenylpyrazole with selected diamines has been applied to derivatives of phenylene-1,2-diamine[2][3] with the intention of studying the influence of a coupling π-system between the pyrazole units on the redox behavior. The investigated systems complete a series of tetrahedrally distorted complexes reported by L. Hennig et al.[4]. The reduction potentials were expected to be strongly dependent on the geometry of the donor sphere surrounding the copper ion but this trend could not be experimentally confirmed by L. Hennig et al. It appeared, therefore, necessary to extend the series by more planar complexes to recognize the trends in the redox properties and reactivity of the singly reduced and oxidized species.

The investigated complexes **1**−**9** belong to the comparatively few examples of stable copper(II) thiolate complexes studied so far.[5] In general, previous research done on these compounds was focused on aspects of biomimetic modelling of the active site behavior of biological *Type I* copper centres with regard to their structural and reduction properties. However, oxidation of these compounds has recieved little attention. Further investigation is required in this field. Notably, the first stable copper(III) thiolate complex [Cu(phmi)](PPh_4)] [phmi = 1,2-phenylenebis(2-mercapto-2-methylpropionamide)] has recently been described in the literature.[6]

Ferraudi and Muralidharan reviewed the photochemistry of copper complexes in 1981.[7] A review of research until the early 1990s is given by Horváth and Stevenson.[8] Only little is known, however, about photochemical properties of

[a] Institut für Anorganische Chemie, Universität Leipzig
Talstraße 35, D-04103 Leipzig, Germany
Fax: (internat.) + 49(0)341/9604600
E-mail: hennigho@sonne.tachemie.uni-leipzig.de
[b] Institute of Molecular Chemistry, Universiteit van Amsterdam
Nieuwe Achtergracht 166, NL-1018 WV Amsterdam,
The Netherlands
Fax: (internat.) + 31-20/525-6456
E-mail: hartl@anorg.chem.uva.nl

  1434−1948/99/0202−0303 $ 17.50+.50/0

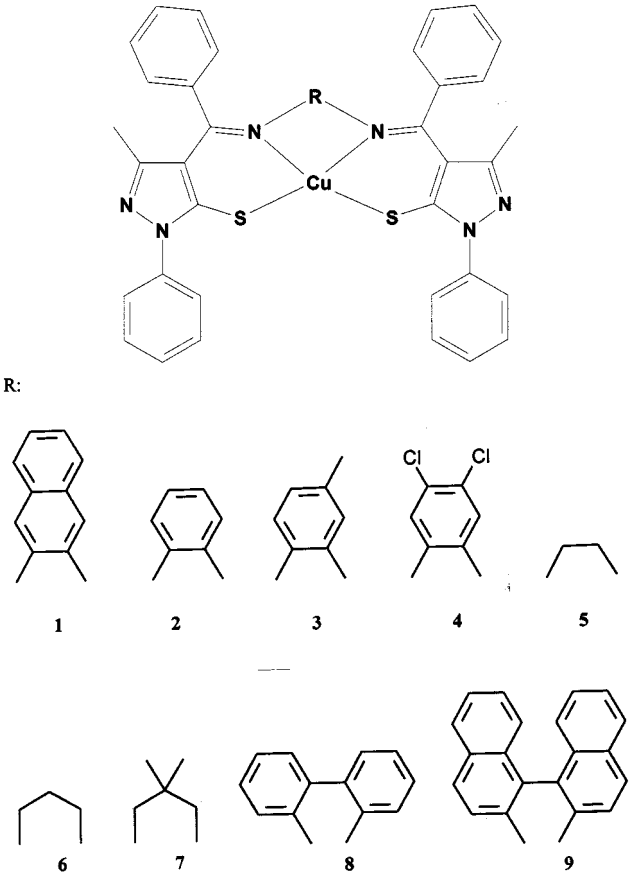

Figure 1. Structural scheme of the Cu^{II} Schiff base complexes used displaying the different backbones R

copper(II) thiolate complexes with large chelating ligands.[9] To our knowledge, only copper(II) complexes with thioethers[10] or dithiolate derivatives (dithiocarbamate,[11−14] maleonitriledithiolate,[15−19] dithiooxalate[20,21] etc.) have been studied photochemically so far.

The detailed spectroscopic and photochemical characterization of large systems like the studied Schiff base complexes **1**−**9** is complicated by strong delocalization of the frontier orbitals and low symmetry.[22] Nevertheless, the presence of intense low-energy charge-transfer absorption bands and the accessibility of two or more oxidation states suggest a variety of photoredox reactions. A redshift of the CT absorptions correlated to the tetrahedral distortion of the CuN_2S_2 moiety is observed.[3] Due to the better separation of the charge-transfer bands, it was important to find out whether redox reactions can be initiated by electronic excitation into the corresponding electronic transitions, or from other excited states, with regard to potential application of these light-sensitive compounds as catalysts in homogeneous photocatalytic systems.[1]

Results and Discussion

Electronic Absorption Spectra

The electronic absorption spectra of the Schiff base ligands employed feature an intense band system in the UV region (see Figure 1). The spectral data of the ligands are listed in Table 1. These transitions are, in accordance with their intensities, attributable to $\pi\rightarrow\pi^*$ transitions within the aromatic system and the azomethine or the thiolate chromophores. They occur at lower energies for the Schiff bases with aromatic coupling between the two imine groups linked by phenylene or biphenylene units. The less intense bands in the near ultraviolet may also arise from $\pi\rightarrow\pi^*$ transitions since they are too intense to be assigned to $n\rightarrow\pi^*$ bands. These absorptions disappear on deprotonation of the ligands during coordination of the metal ion.

Table 1. UV/Vis-spectroscopic data of the free ligands $\mathbf{H}_2$**1**−$\mathbf{H}_2$**9** in $CHCl_3$ at 293 K

Ligand	Band λ_{max} [nm] (ε [$M^{-1}cm^{-1}$])
$\mathbf{H}_2$**1**	271 (37300), 321 (34000), 419 (11700)
$\mathbf{H}_2$**2**	276 (35500), 318 (35800), 421 (11900)
$\mathbf{H}_2$**3**	275 (34800), 317 (35100), 419 (12300)
$\mathbf{H}_2$**4**	271 (36000), 321 (36000), 426 (10900)
$\mathbf{H}_2$**5**	277 (26100), 314 (31200), 399 (11700)
$\mathbf{H}_2$**6**	281 (24500), 310 (29900), 394 (11100)
$\mathbf{H}_2$**7**	282 (25600), 311 (31200), 394 (11400)
$\mathbf{H}_2$**8**	271 (32800), 321 (26300), 419 (10600)
$\mathbf{H}_2$**9**	284 (37900), 344 (28300), 446 (12100)

The electronic absorption spectra of the copper(II) complexes **1**−**9** exhibit UV absorption bands that can be assigned to intraligand (IL) transitions. They are only slightly shifted relative to those of the corresponding uncoordinated Schiff base ligands (Table 2). The UV/Vis region displays bands or shoulders which have been assigned to ligand-to-metal (σ,π-SR$\rightarrow Cu^{II}$) charge-transfer transitions (LMCT)[4] as reviewed by Schugar.[37] For example, **5** shows a shoulder at 346 nm and a relatively strong and broad absorption at 438 nm with a shoulder at 520 nm. In contrast to that, two intense bands in the visible region are observed for **9** (530 nm and 659 nm), together with a shoulder at 355 nm (Table 2). These bands exhibit a red shift on going from a square-planar to a pseudotetrahedral geometry of the CuN_2S_2 chromophores, i.e. from **1** to **9**.[22,29] It should be recalled that strict assignment cannot be given due to strong delocalization of the frontier orbitals.[22]

Ligand field transitions (LF or d-d) at Cu^{II} could not be localized due to strong overlap with CT bands in the visible region. This is not surprising, as the LF transitions are also expected to shift to lower energy with increasing tetrahedral distortion.[30,33]

Cyclic Voltammetry

Cyclic voltammograms of the complexes **1**−**9** were recorded in butyronitrile, as this solvent is also suitable for spectroelectrochemical studies at variable temperatures (described hereinafter). In selected cases THF was employed. All complexes **1**−**9** can be oxidized and reduced within the

Table 2. UV/Vis-spectroscopic data of the complexes **1**−**9** and their redox products

Complex[a]	Band λ_{max} [nm] (ε [in $M^{-1}cm^{-1}$])
1[a]	476, 410 (sh), 328, 273
1[b]	484 (sh) (4300), 410 (sh) (16200), 336 (41600), 275 (41400)
1(ir)[b][c]	400 (sh) (5100), 310 (sh) (29700), 250 (65800)
1(io)[b][c]	350 (sh) (10700), 270 (sh) (39500), 208 (61200)
2[a]	500 (sh) (2500), 405 (sh) (11900), 344 (32900), 275 (37500)
2[b]	480 (sh), 460(sh), 375 (sh), 323, 256
2(ir)[b][c]	390 (sh) (2100), 280 (sh) (23800), 233 (48800)
2(io)[b][c]	331 (sh) (7200), 240 (sh) (32500)
2(r)[b][c]	510 (sh) (1000), 420(sh), 330 (sh) (13800), 275 (sh), 234 (46200)
2(o)[b][c]	750 (sh) (1800), 628 (2500), 516 (5100), 439 (5000), 375 (sh), 330 (30900), 262 (34800), 239 (34200)
3[a]	500 (sh) (2500), 410 (sh) (12200), 345 (33600), 277 (39400)
4[a]	505 (sh) (2500), 410 (sh) (14100), 350 (33700), 317 (28400), 279 (34000)
5[a]	520 (sh) (1600), 438 (3500), 346 (sh) (10800), 275 (35600)
5[b]	500 (sh), 420, 330 (sh), 275
5(r)[b,c]	390 (sh) (3400), 330 (sh), 270 (36100)
5(o)[b,c]	> 900, 556 (1400), 432 (10100), 270 (sh) (15000), 251 (35900)
6[a]	610 (sh) (1900), 476 (3900), 339 (12100), 274 (36700)
6[b]	580, 473, 350 (sh), 322, 269, 224
6(r)[b,c]	440 (sh) (900), 330 (sh) (1200), 263 (39400)
6(o)[b,c]	800 (2900), 550 (sh) (1800), 449 (9900), 340 (sh) (5900), 280 (sh) (24700), 250 (45400)
7[a]	599 (1900), 473 (3700), 341 (11500), 272 (35500)
8[a]	630 (sh) (1400), 522 (2100), 350 (sh) (10800), 279 (35500)
9[a]	659 (1600), 530 (1800), 355 (sh) (17000), 290 (51800)
9[b]	660, 511, 375 (sh), 334, 290
9(r)[b,c]	440 (sh) (2100), 350 (sh), 272 (32800)
9(o)[b,c]	733 (2600), 570 (sh), 469 (3900), 330 (sh) (15600), 290 (sh) (38900), 276 (39200)

[a] In $CHCl_3$ at 293 K. − [b] In butyronitrile containing $3\cdot10^{-1}$ M Bu_4NPF_6 at 293 K. − [c] Abbreviation **(ir)** denotes the secondary reduction products, **(r)** the primary one-electron reduction products, **(io)** the secondary oxidation products, and **(o)** the primary one-electron oxidation products.

Table 3. Electrochemical data of the complexes **1**−**9**[a]

Complex	$E_{p,c}$(red)	ΔE_p	$E_{p,a}$(ox)	ΔE_p	ΔE_p(Fc/Fc$^+$)
Butyronitrile					
1	−1.03[b]	−	0.31[b]	0.105	0.100
1[d]	−1.05[b]	0.130	0.28[e]	0.100	0.100
1(ir)	−	−	−0.30[b]	−	
1(ir)[e]	−	−	−0.20[b]	−	
2	−1.04[b]	−	0.34[b]	0.095	0.105
2[d]	−0.96[e]	0.175	0.27[e]	0.100	0.100
2(ir)	−	−	−0.30[b]	−	
3	−1.06[b]	−	0.32[b]	0.100	0.105
3[d]	−1.08[b]	0.110	0.25[e]	0.100	0.100
3[e]	−1.06[e]	0.125	0.30[e]	0.100	0.100
3(ir)	−	−	−0.32[b]	−	
4	−0.94[b]	−	0.42[b]	0.110	0.105
4[d]	−0.98[b]	0.110	0.37[e]	0.100	0.100
4[e]	−0.99[e]	0.150	0.35[e]	0.110	0.100
4(ir)	−	−	−0.26[b]	−	
4(ir)[e]	−	−	−0.24[b]	−	
5	−1.23[e]	0.130	0.27[e]	0.115	0.105
6	−1.04[e]	0.110	0.23[b]	−	0.100
6[d]	−1.06[e]	0.175	0.21[e]	0.150	0.110
7	−1.02[e]	0.110	0.24[b]	−	0.110
7[d]	−0.97[e]	0.100	0.28[b]	0.150	0.100
8	−0.89[e]	0.100	0.25[b]	−	0.100[g]
8[f]	−0.81[e]	0.100	0.30[b]	0.140	0.105[g]
9	−0.84[e]	0.100	0.29[b]	−	0.100
9[e]	−0.80[e]	0.100	0.28[e]	0.150	0.090
THF					
2	−1.19[b]	−	0.37[e]	0.100	0.100
2(ir)	−	−	−0.36[b]	−	
6	−1.08[e]	0.110	0.31[e]	0.110	0.110
9	−0.95[e]	0.110	0.30[e]	0.110	0.110

[a] Cyclic voltammetry, $5\cdot10^{-4}$ M solutions of the complexes in butyronitrile or THF containing $3\cdot10^{-1}$ M Bu_4NPF_6, T = 293 K (unless stated otherwise), Pt disk electrode (0.42 mm^2 apparent surface area), scan rate v = 100 mV/s. Redox potentials given vs. $E_{1/2}$(Fc/Fc$^+$) = 0.43 V and 0.57 V vs. SCE in butyronitrile and THF, respectively. Abbreviation **(ir)** denotes the secondary reduction products of **1**−**4**, oxidizable back to the parent complexes. − [b] Chemically irreversible redox process. − [c] T = 213 K. − [d] T = 230 K. − [e] Chemically reversible redox process. − [f] T = 250 K. − [g] $CoCp_2^{+/0}$ employed as internal standard redox system ($E_{1/2}$ = −1.34 V vs. Fc/Fc$^+$). −

potential window available in these solvents. The corresponding redox potentials (vs. Fc/Fc$^+$) are summarized in Table 3. The representative cyclic voltammograms of **2**, **5**, and **9** in butyronitrile are shown in Figures 2A−C, respectively. The cathodic and anodic steps will be described separately.

Reduction

In *butyronitrile*, the reduction of the complexes **5**−**9** on the time scale defined by scan rates $v \geq 50$ mV/s is chemically reversible already at room temperature (see Figure 2C). The electron transfer is electrochemically reversible for **7**−**9**, but quasi-reversible for **5** and **6** (see Figure 2B and Table 3). On the other hand, the reduction of the complexes **1**−**4** at room temperature is chemically totally irreversible, as no anodic counterpeak was observed on the reverse anodic scan (see Figure 2A). The reduction in the latter case produces species, denoted **1(ir)**−**4(ir)** in Table 3, which oxidize on the reverse scan ca. 0.7 V more positively in comparison with the reduction potentials of the parent complexes **1**−**4**. The complexes **1**−**9** could be reduced completely with one equivalent of cobaltocene, which agrees with the transfer of one electron. The cobaltocenium salts of the anionic products **5(r)**−**9(r)** persisted in the solution for several minutes without any decomposition and could be oxidized back completely to parent **5**−**9** by one equiva-

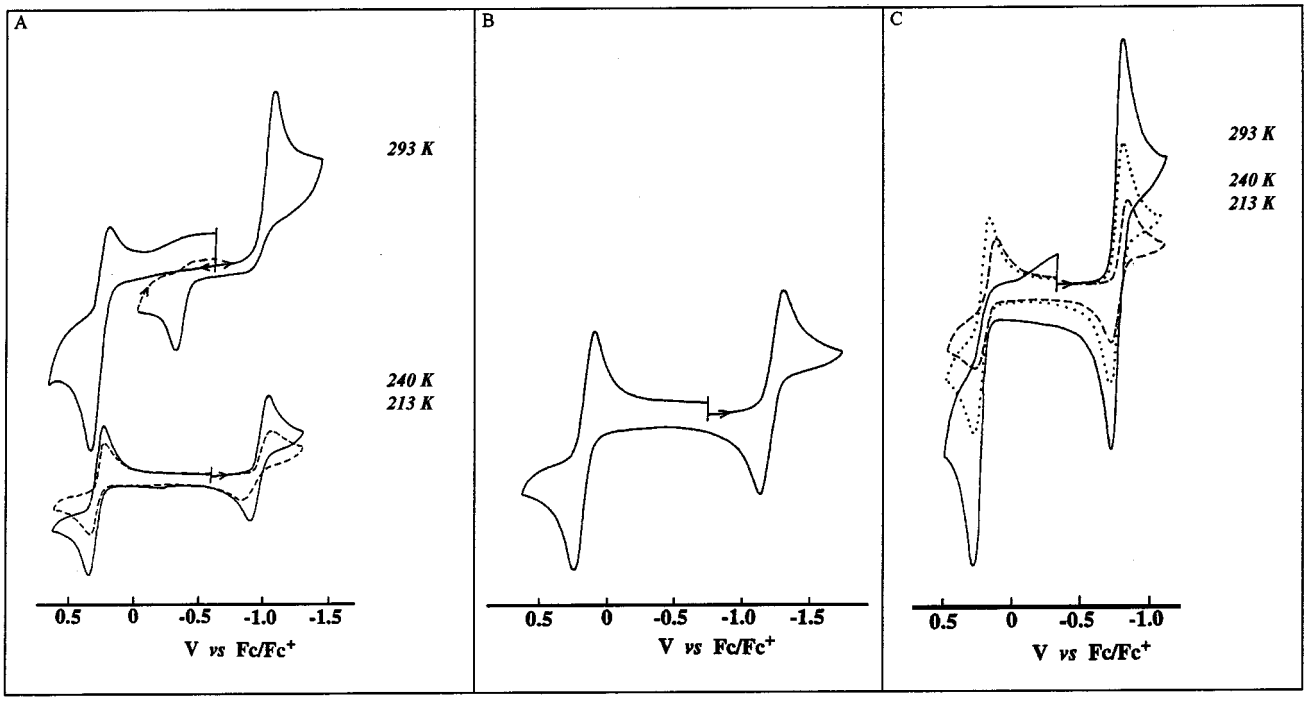

Figure 2. Cyclic voltammograms of the complexes (A) **2** at 293, 240, and 213 K; (B) **5** at 293 K; (C) 9 at 293, 240, and 213 K (butyronitrile/ $3 \cdot 10^{-1}$ M Bu_4NPF_6, Pt disk microelectrode with 0.42 mm^2 disk area, scan rate v = 100 mV/s)

lent of $FcBF_4$. The secondary anionic reduction products **1(ir)**−**4(ir)** are also inherently stable, as confirmed by cyclic voltammetry. Scan reversal beyond their anodic peaks (see Table 3) led to the reappearance of the cathodic peaks due to the reduction of **1**−**4**. The recovery of **1** and **2** on oxidation of **1(ir)** and **2(ir)**, respectively, was further documented by corresponding UV/Vis spectroelectrochemical experiments (see below). This behavior points to rapid conversion of the primary one-electron reduction products **1(r)**−**4(r)** to **1(ir)**−**4(ir)** at room temperature, resulting in a reversible conformational change (see below). Oligomerization or polymerization reactions induced by the reduction are less likely due to the limited conformational flexibility of the ligand framework in the parent complexes **1**−**4** (see Figure 1). As reported recently by Rasmussen et al.,[34] a tetranuclear cluster (Cu_4L_4) is produced in the course of the reaction between the more flexible deprotonated ligand *N*,*N*′-(2,2′-biphenyldiyl)bis(4-aminomethyl-1,3-diphenyl-5-thiopyrazole) and $[Cu(CH_3CN)]^+$ in DMF.

All stable reduction products **1(ir)**−**4(ir)** and **5(r)**−**9(r)** are EPR-silent. This result is consistent with the formation of one-electron-reduced, formal Cu^I complexes; although, the Extended-Hückel calculations on the fragments of the parent complexes **2**, **5**, and **6** and the average imine N−C distances (1.31 Å for **8**[3,14]) in the middle of the N=C/N−C bond-length range[38] (1.25−1.39 Å) show that the singly occupied redox orbital (SOMO) is strongly delocalized over the *cis*-CuN_2S_2 moiety.[22] It cannot be excluded, however, that in the anionic reduction products **1(r)**−**9(r)** the added electron density resides more on the central Cu atom, for example due to the mixing of the HOMO of the anions with close-lying empty orbitals (LUMO and LUMO +1) which are largely localized[22] on the electron-withdrawing imine functions and the thiopyrazolone rings.

Within the series of the parent compounds **1**−**9** the geometry around the central ion strongly depends on the flexibility of the backbone R connecting the two imine nitrogen atoms (see Figure 1). Thus, the rather rigid naphthylene and phenylene backbones in **1**−**4** impose only slightly distorted square planar geometry, as documented by the crystal structures of **1** and **2** showing θ = 3.3° and 9.3°, respectively (θ is the dihedral angle between the two N−Cu−S planes in the crystal). In contrast to this, in **5** and **6** with the more flexible ethylene and propylene backbones, the value for θ increases to 34.7° and 42.5°, respectively, and θ = 52.1° was determined for **8** (L. Hennig et al.[4]) with the flexible 2,2′-biphenylene backbone enforcing a large tetrahedral twist on the coordination polyhedron. Even larger tetrahedral distortion from the planar geometry was recently observed for a novel complex **10** with the backbone R = butylene, where θ = 56°.[36] In general, Cu^I complexes will prefer the tetrahedral coordination, which also applies for the studied primary one-electron reduction products **1(r)**−**9(r)**. We have indeed observed that the one-electron reduction at room temperature is chemically irreversible for the nearly square planar complexes **1**−**4**, while the thermal stability of **5(r)**−**9(r)** nicely correlates with the increased tetrahedral distortion in **5**−**9**. We therefore propose that the secondary chemical reactivity of **1(r)**−**4(r)** producing **1(ir)**−**4(ir)** has its origin in a tetrahedral twist induced by the electron-transfer step. The electrochemically quasireversible character of the reduction of **5** at room temperature may indicate some small conformational change on going to **5(r)** while the geometry of the

coordination polyhedron of **6(r)**−**9(r)** with respect to that of the parent complexes **6**−**9** remains unchanged. It is noteworthy that the size of the chelate ring, the nature (aromatic, aliphatic) and steric demands of the bridging system in **1**−**7** possess rather limited influence on the reduction potential. Only for the pseudotetrahedral complexes **8** and **9** an apparent positive shift of the reduction potential was observed (see Table 3). This shift may arise from a stabilizing overlap between the π systems of the twisted 2,2′-biphenylene and 2,2′-binaphthylene backbones, respectively, and the π system of the "4-benzyl" substituent at the thiopyrazolone rings, as judged from the crystal structure of **8**.[4,35] For example, the tetrahedrally most twisted complex **10** with the aliphatic butylene backbone R reversibly reduces at $E_{p,c} = -1.03$ V,[36] i.e. again more negatively than **8** and **9** but identical to nearly planar **1**−**3** and less twisted **6** and **7**.

Cyclic voltammetry performed at moderate scan rates has revealed that the reduction of **2** becomes chemically reversible at $T = 230$ K, as judged from $I_{p,a}/I_{p,c} = 1$ and disappearance of the anodic peak due to the oxidation of **2(ir)** on the reverse scan. Between 243 and 213 K the ΔE_p value gradually increases relative to that of the Fc/Fc^+ internal standard and the voltammetric response broadens, while $I_{p,a}/I_{p,c}$ again becomes less than 1 and $I_p v^{-1/2}$ is virtually independent of v (see Figure 2A). This behavior is characteristic for an electrochemically quasireversible charge transfer and suggests that, likewise **5(r)** and **6(r)** (see above), also **2(r)** and parent **2** may slightly differ in the coordination geometry. A similar temperature dependent voltammetric response was recorded for **3** and **4**; chemical reversibility of the reduction in the latter cases was, however, only achieved at $T = 213$ K (see Table 3). In contrast to this, the one-electron reduction of the nearly square planar complex **1** ($\theta = 3.3°$) remains chemically irreversible even at $T = 213$ K.

No significant difference in the reduction path was observed when cyclic voltammograms of **2**, **6**, and **9** were recorded in *THF* at $T = 293$ K, besides a shift of the reduction potentials to lower values by 40−160 mV (see Table 3).

Oxidation

Oxidation of **1**−**9** in *butyronitrile* occurs, independently of the geometry of the CuN_2S_2 core, in a narrow potential range (see Table 3). At $v = 100$ mV/s oxidation of the nearly square planar complex **1**, in contrast to its reduction, is a both chemically and electrochemically reversible one-electron process independently of the applied temperature between 293 and 213 K. Of course, at $T = 330$ K for example, the oxidized species of **1** will decompose. In consequence of the increasing tetrahedral distortion of the coordination polyhedron, the oxidation of the complexes **2**−**10** at $T = 293$ K is chemically irreversible at $v = 100$ mV/s (see Table 3). The oxidation of the complexes **2**−**4** on this subsecond time scale is still an one-electron process and the primary oxidation products **2(o)**−**4(o)** are detectable on the reverse anodic scan ($I_{p,c}/I_{p,a} \approx 0.4-0.5$). At $T = 255$ K the secondary chemical reactivity of **2(o)**−**4(o)** becomes completely suppressed, as judged from $I_{p,c}/I_{p,a} = 1$ (see Figure 2A). The one-electron-oxidized complex **5(o)** does not fit within the series, being exceptionally stable even at room temperature (see Figure 2B). On the other hand, complex **6** is oxidized in a chemically totally irreversible step which corresponds with transfer of two electrons ($n_{app} = 2$). Proceeding to **7**−**9** the oxidation remains chemically irreversible but the number of transferred electrons at $v = 100$ mV/s again decreases to $n_{app} \approx 1.5$ for **7** and $n_{app} = 1$ for **8** and **9** (see Figure 2C). Scanning at low temperatures revealed that the oxidation of **6** at $T = 230$ K becomes chemically reversible ($n_{app} = 1$) while for **9** $T = 220$ K is required to stabilize the cation **9(o)** at $v = 100$ mV/s. The corresponding cations **7(o)** and **8(o)** remain unstable even at $T = 213$ K. It is noteworthy that, opposite to **1**−**4**, the one-electron oxidation of **6**−**9** producing **6(o)**−**9(o)** is electrochemically quasireversible while the one-electron reduction of these complexes under identical conditions is electrochemically reversible (see Table 3). This redox behavior may indicate that, likewise **1**−**4** and **1(r)**−**4(r)** (see above), also **6**−**9** and **6(o)**−**9(o)** in butyronitrile slightly differ in the coordination geometry of the CuN_2S_2 core. In the case of **5** the little conformational change applies both for **5(r)** and **5(o)**.

In sharp contrast to the cyclic voltammetric response in butyronitrile, the complexes **2**, **6**, and **9** oxidize in THF at room temperature in a both chemically and electrochemically reversible one-electron step (see Table 3). Addition of an excess of PPh_3 to the THF solution of **9** converts the oxidation of the latter complex to a chemically totally irreversible two-electron process while the chemically reversible one-electron reduction remains unaffected.

The one-electron-oxidized complexes **1(o)**−**9(o)** can be viewed in first approach formally as d^8-Cu^{III} species. Their preference for the square-planar geometry of the CuN_2S_2 polyhedron may explain the electrochemically quasireversible character of the one-electron oxidation of the strongly tetrahedrally distorted parent complexes **5**−**9**. This description is, however, too oversimplified as the SOMO of **1**−**9** is known to be strongly delocalized over the whole CuN_2S_2 moiety, with a major contribution from the two sulfur atoms.[22] For example, oxidation of the derivative of **2** with the thiolate donors replaced by oxygen functions occurs significantly more positively [**2-O**: $E_{p,a}(ox) = 0.9$ V and $E_{p,c}(red) = -1.38$ V vs. Fc/Fc^+ in butyronitrile at $T = 293$ K; the one-electron reduction is chemically reversible at $v = 100$ mV/s]. It can therefore be accepted that the one-electron oxidation mainly affects the stability of the Cu−S bond(s). The chemical irreversibility of the oxidation and its overall two-electron character have probably its origin in the cleavage of the Cu−S bonds, followed by closure of intra- or intermolecular disulfide S−S bonds in **1(io)**−**9(io)**, the secondary oxidation products. The latter processes become significantly accelerated for the tetrahedrally twisted complexes **6**−**9**, pointing to the role of conformational change induced by the electron transfer to the anode, and

in the presence of strongly coordinating ligands like butyronitrile or PPh_3, which may occupy the coordination sites abandoned by the sulfur atoms. This anodic path explains the increased chemical reversibility of the primary one-electron oxidation step in weakly coordinating THF.

UV/Vis Spectroelectrochemistry

UV/Vis spectra of primary and secondary redox products of **1**−**9**, detected by cyclic voltammetry were recorded in situ at variable temperatures by using appropriate OTTLE cells. The main goal of these experiments was to obtain spectroscopic information needed for correct assignment of species generated on photo-induced reduction and oxidation of selected complexes under study. The UV/Vis spectroelectrochemical data are collected in Table 2.

Reduction

The one-electron reduction of **5** (Figure 3A), **6** and **9** (Figure 3B) in butyronitrile at 293 K, and **2** in butyronitrile at 190 K (Figure 3C) in the course of the OTTLE experiments yielded the stable species **5(r)**, **6(r)**, **9(r)**, and **2(r)** as single products. This assignment was based on the thin-layer cyclic voltammograms recorded during the reduction and reverse reoxidation steps, which corresponded with the chemically reversible redox couples observed in ordinary cyclic voltammograms under identical conditions. In all of these cases retention of isosbestic points was observed and the reoxidation of the anionic products resulted in full recovery of the parent complexes. The UV/Vis spectra of the anions are characterized by the presence of an intense band between 230 and 275 nm with an apparent shoulder at ca. 330 nm. The charge-transfer absorption bands of the parent complexes in the visible region disappeared. Instead, the anions **2(r)**, **5(r)**, **6(r)**, and **9(r)** absorb only weakly between 380 and 500 nm.

The UV/Vis spectrum of square-planar **2(r)** also shows a weak absorption at 510 nm (see the insert to Figure 3C). This band is missing in the UV/Vis spectrum of the secondary reduction product **2(ir)** generated during the one-electron reduction of **2** in butyronitrile at 293 K (see Figure 3C). The rest of the UV/Vis spectrum of **2(ir)** closely resembles that of **2(r)**, pointing to a very similar bonding situation in both anions. For example, oxidation at the positively shifted anodic potential of **2(ir)** (see Table 3) also led to the complete reappearance of the UV/Vis spectrum of **2**, in agreement with the cyclic voltammetric behavior (see above). Almost identical spectroscopic responses were observed for the chemically irreversible one-electron reduction of nearly square planar **1** at 293 K and for the reverse oxidation of **1(ir)** (see Table 2 and Figure 3C).

Oxidation. Electrochemical oxidation of **2**, **5**, **6**, and **9** in butyronitrile at 193 K within the UV/Vis OTTLE cell produced stable cations **2(o)**, **5(o)**, **6(o)**, and **9(o)**. As depicted in Figure 4 and summarized in Table 2, the electronic absorption spectra of these cations typically exhibit several

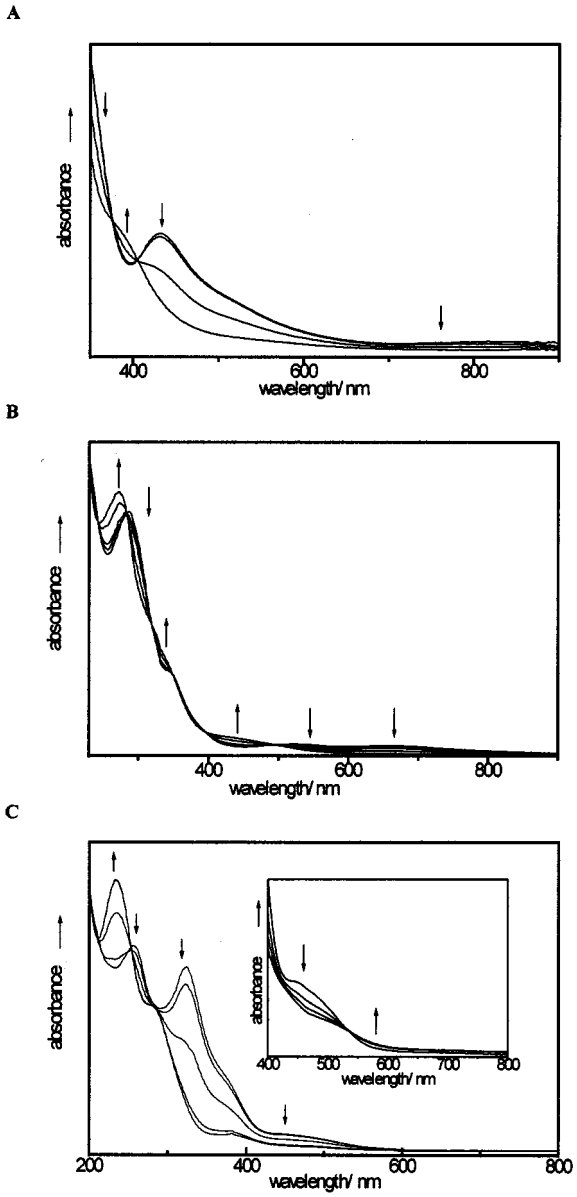

Figure 3. UV/Vis-spectroscopic changes accompanying electrochemical reduction of **5** (A), **9** (B), and **2** (C) in butyronitrile at 293 and 193 K (inset) within an OTTLE cell[27,28]

absorption bands covering the whole visible region between 400 and 900 nm. Their assignment was not attempted, particularly due to the strong electronic delocalization of the parent complexes, which probably also persists in the one-electron-oxidized species. The cation **2(o)** was still observable at 230 K whereas **5(o)** existed a few minutes even at 293 K. The oxidation of **2** at room temperature only yielded the stable secondary product **2(io)** which does not absorb in the visible region (see Table 2). Interestingly, reverse reduction of **2(io)** directly resulted in full recovery of the parent complex **2**. The same result was obtained for the corresponding planar complex **1**, regardless of the chemically reversible one-electron oxidation of the latter complex at 293 K on the subsecond time scale of cyclic voltammetry. Provided **1(io)**−**9(io)** contain intra- or intermolecular disulfide linkages, as argued above, their reduction is then largely

localized on this function, resulting in rapid recoordination of the reduced thiolate appendages and the recovery of **1**−**9**.

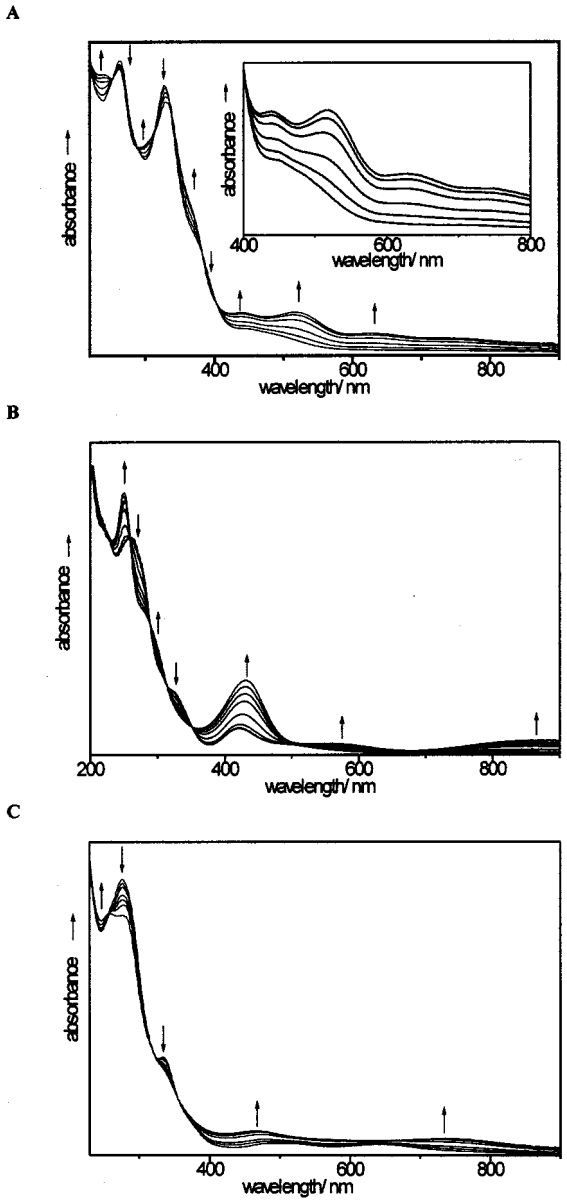

Figure 4. UV/Vis-spectroscopic changes accompanying electrochemical oxidation of **2** (A), **5** (B), and **9** (C) in butyronitrile at 193 K within an OTTLE cell[28]

Photochemistry

The photochemical experiments have been carried out to investigate the possibility to initiate photoinduced electron-transfer processes producing oxidized or reduced species from the parent copper(II) complexes.

Photoreduction

Continuous photolysis of complexes **1**−**9** with full output of the mercury lamp in donor solvents EtOH or THF at room temperature led to bleaching of the bands in the visible region within approximately 30 min. Identical spectral changes were monitored when wavelengths λ_{irr} < 310 nm were excluded. The photoreactions became accelerated in the presence of electron donors such as $N(CH_2CH_2OH)_3$ (TEA). No photoreduction took place in *t*BuOH within 30 min (T = 303 K), presumably because this solvent does not liberate α-hydrogen atoms, in contrast to THF and EtOH.

The UV/Vis-spectral changes accompanying the photoreduction of complex **9** at 293 K are depicted in Figure 5A (λ_{irr} > 315 nm). Identical spectral changes were monitored upon the electrochemical one-electron reduction of this complex within the OTTLE cell. The same behavior was observed for **8**. The increase of absorbance around 450 nm is a characteristic feature of the primary reduced anions **8(r)** and **9(r)**. The conversion is complete within ca. 60 min. The photoreduction requires strictly anaerobic conditions. Full recovery of the starting complexes was observed on air exposure of the photogenerated anions **8(r)** and **9(r)** if the irradiation was stopped before side reactions started.

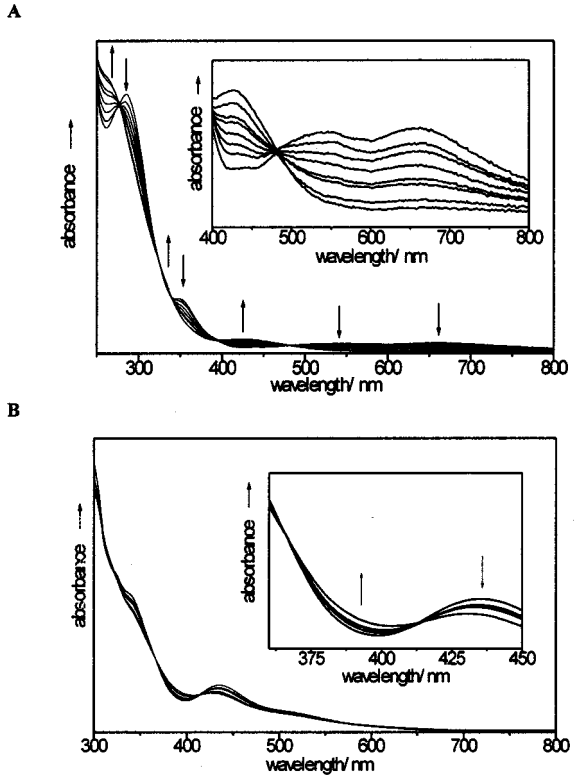

Figure 5. UV/Vis-spectroscopic changes accompanying continuous photolysis of **9** (A) at 293 K, **5** (B) at 193 K in THF (λ_{irr} > 310 nm, t_{irr} = 0, 10, 20, 35, 50, 70 s)

Photochemical generation of the reduced complexes **5(r)**−**7(r)** failed at room temperature, though the spectroelectrochemical investigations reveal their thermal stability. Continuous photolysis in THF at low temperatures ($T \leq$ 213 K), however, yielded the expected anionic complexes. The formation of **5(r)** at T = 193 K is shown in Figure 5B.

The application of low temperature was not successful in the case of **2(r)**. The absence of the weak absorption of **2(r)** at 500 nm arising in the course of the electrochemical

reduction, reveals that only the secondary product **2(ir)** was formed on irradiation of **2** in EtOH and THF, even at T = 193 K. This finding obviously fits with the lower stability of the primary reduced complex **2(r)** in comparison with **5(r)−9(r)**, as discussed in previous sections.

Photooxidation

Irradiation of **1**−**9** in $CHCl_3$ at 546, 436, and 366 nm did not lead to any measurable photoreaction, although intense CT absorption bands dominate in this region (see Table 2). With λ_{irr} = 332 nm only minor spectral changes could be detected within 60 min. A considerable acceleration of the photoreaction was observed when shorter irradiation wavelengths (λ_{irr} = 313 , 302 , and 254 nm) were applied, though the absorbance of **1**−**9** does not deviate significantly at the latter wavelengths from that at 334 or 366 nm. Notably, a week absorbance ($A \approx 0.004$ vs. H_2O; d = 1 cm) of the solvent $CHCl_3$ was measurable already at λ = 313 nm (cut off at ca. 250 nm).

Continuous photolysis (λ_{irr} = 254 , 302 , and 313 nm) of the complexes **1**−**9** in $CHCl_3$ only resulted in disappearance of the visible and UV absorption bands. The bleaching reactions may indicate formation of secondary oxidized products as studied in the course of the corresponding UV/Vis-spectroelectrochemical experiments (see Table 2).

In order to obtain evidence for the formation of the primary one-electron-oxidized species **1(o)**−**9(o)** upon irradiation in $CHCl_3$, flash photolysis experiments were carried out at room temperature. The samples were excited with 266 nm and 355 nm laser pulses. The ns transient absorption spectra were recorded in 10-nm steps for deaerated, as well as oxygen-saturated solutions (Figure 6). The expected increase of absorption in the visible region due to the cationic species **1(o)**−**9(o)** was indeed observed independent of the exclusion of oxygen, as displayed in Figure 7 for **2**. Following the decay of this transient absorption on the ns time scale showed that the cationic complexes exist at room temperature only a few hundred ns. The lifetimes τ of **1(o)**−**9(o)** in oxygen-free $CHCl_3$ were estimated assuming a first- or pseudo-first-order decay. Values for τ are given in Table 4. The longer lifetimes of **2(o)** and particularly **1(o)** relative to those of **6(o)**, **9(o)**, and particularly **8(o)** nicely agree with the cyclic voltammetric trends (see above).

In general, the photochemical reactivity of **1**−**9** in $CHCl_3$ tracks the absorbance spectrum of the solvent $CHCl_3$. The observed reactions are therefore assigned to be solvent initiated or to take place from CTTS excited states, which are not manifested in the electronic spectrum of these compounds in $CHCl_3$.[38]

No spectral changes could be monitored on excitation of the complexes **1**−**9** with visible light (λ > 400 nm) within 30 min. This behavior appears to be a result of relaxation processes from CT excited states via LF excited states.

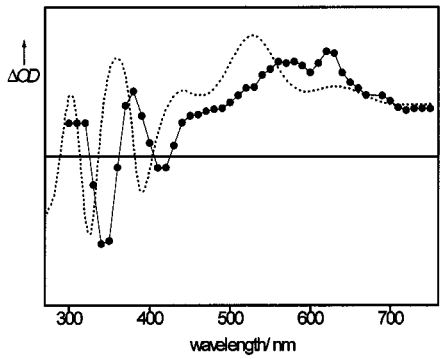

Figure 6. Transient absorption spectrum of **2** in $CHCl_3$ measured point-by-point 0.4 μs after laser excitation at 266 nm (••••), compared with UV/Vis absorbance difference spectrum recorded on one-electron oxidation of **2** in *butyronitrile* at 193 K (----) (see also Figure 3C)

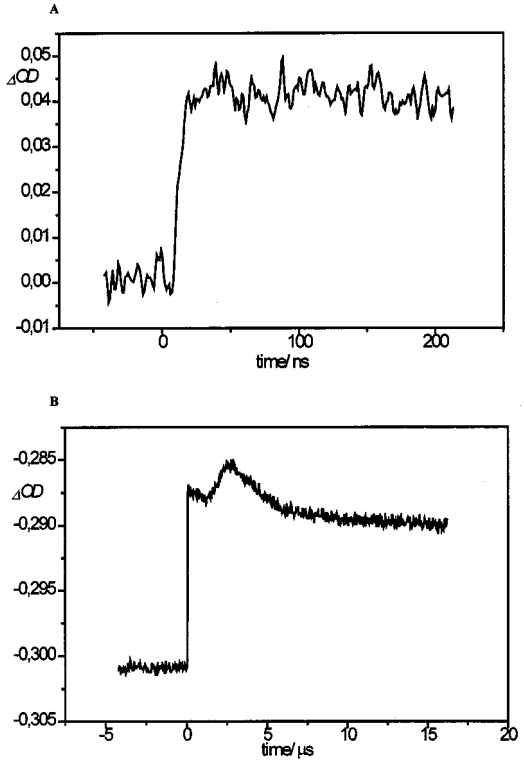

Figure 7. Transient decay following flash excitation of **2** in $CHCl_3$ at 266 nm on nanosecond (A) and microsecond (B) time scales

Table 4. Estimated lifetimes τ of the photooxidized complexes

Cation	**1(o)**	**2(o)**	**5(o)**[a]	**6(o)**	**8(o)**	**9(o)**
τ [μs]	3.1	1.2	–	0.5	0.2	1.0

[a] The lifetime of **5(o)** could not be estimated due to very weak decrease of optical density accompanying the formation of secondary product sfrom **5(o)**.

Conclusions

The thiolate sulfur atom of the complexes under study is bound to an sp^2-hybridized carbon atom. The coupling of the pyrazole-ring carbon atom and the sulfur p-orbitals provides an easily conjugable framework to stabilize the thiolato copper(II) linkage. This electronic coupling results in a strong delocalization crucially influencing the electro-

chemical and photochemical properties of **1**−**9**. This kind of strong delocalization seems to be responsible that photochemical reactions can only be initiated by exciting intraligand excited states whilst excitation of low-energy electronically excited states leads to fast radiationless deactivation via d-d excited states.

Both thermally and photochemically induced reaction pathways of **1**−**9** are summarized in Scheme 1. In general, the same primary redox products, as studied by spectroelectrochemistry, are initially formed on photolysis in the appropriate reducing and/or oxidizing media. Photoreduction occurs in solvents bearing H_α atoms. Photooxidation in chlorinated solvents like $CHCl_3$ are solvent-initiated or initiated by population of CTTS-excited states.

The oxidation takes place on the copper−sulfur moiety. Obviously, the strong delocalization is responsible for the similar values of the oxidation potentials. The primary one-electron-oxidized products of copper(II) thiolate complexes could be characterized by UV/Vis spectroscopy at low temperature.

The reduction behavior is strongly dependent on the geometry of the pseudotetrahedral N_2S_2 donor set surrounding the Cu^{II} ion. The stability of the primary one-electron-reduced products increases with stronger tetrahedral distortion. An opposite trend applies for the primary one-electron-oxidized species (formally d^8-Cu^{III}) which prefer square-planar geometry of the coordination sphere.

The effect of different substituents on the redox behavior of the nearly planar complexes **1**−**4** containing aromatic backbones is not significant. The influence of the ligand flexibility on the reduction of the complexes with aliphatic backbones is reflected in the two-electron oxidation of the complexes **6** and **7** in comparison with **8** and **9** on the time scale of cyclic voltammetry. The oxidation path is significantly influenced by the kind of donor solvents used. Thus, strongly coordinating butyronitrile facilitates cleavage of the Cu−S bonds in the primary one-electron-oxidized species, followed by transfer of a second electron. This reactivity can be supressed in weakly coordinating THF.

Experimental Section

Synthetic Methods and Materials: All chemicals were of analytical grade and were used as received from Aldrich [Bu_4NPF_6, ferrocene (Fc), cobaltocene ($CoCp_2$), cobaltocenium hexafluorophosphate ($CoCp_2PF_6$), PPh_3]. Ferrocenium tetrafluoroborate ($FcBF_4$) was prepared according to a literature procedure.[23] THF (Acros) was dried with NaOH pellets, followed by distillation from Na/benzophenone under nitrogen. Butyronitrile (Fluka) was freshly distilled from CaH_2 under nitrogen. Solvents for photoredox reactions ($CHCl_3$, ethanol), from Merck (Uvasol) or Aldrich (*t*BuOH), were degassed by means of ultrasound or bubbling solvent-saturated N_2 through the solutions before use. The complexes **1**−**9** (Figure 1) were synthesized according to literature procedures.[2,4,22] Their purity was checked by elemental analysis and mass spectrometry.

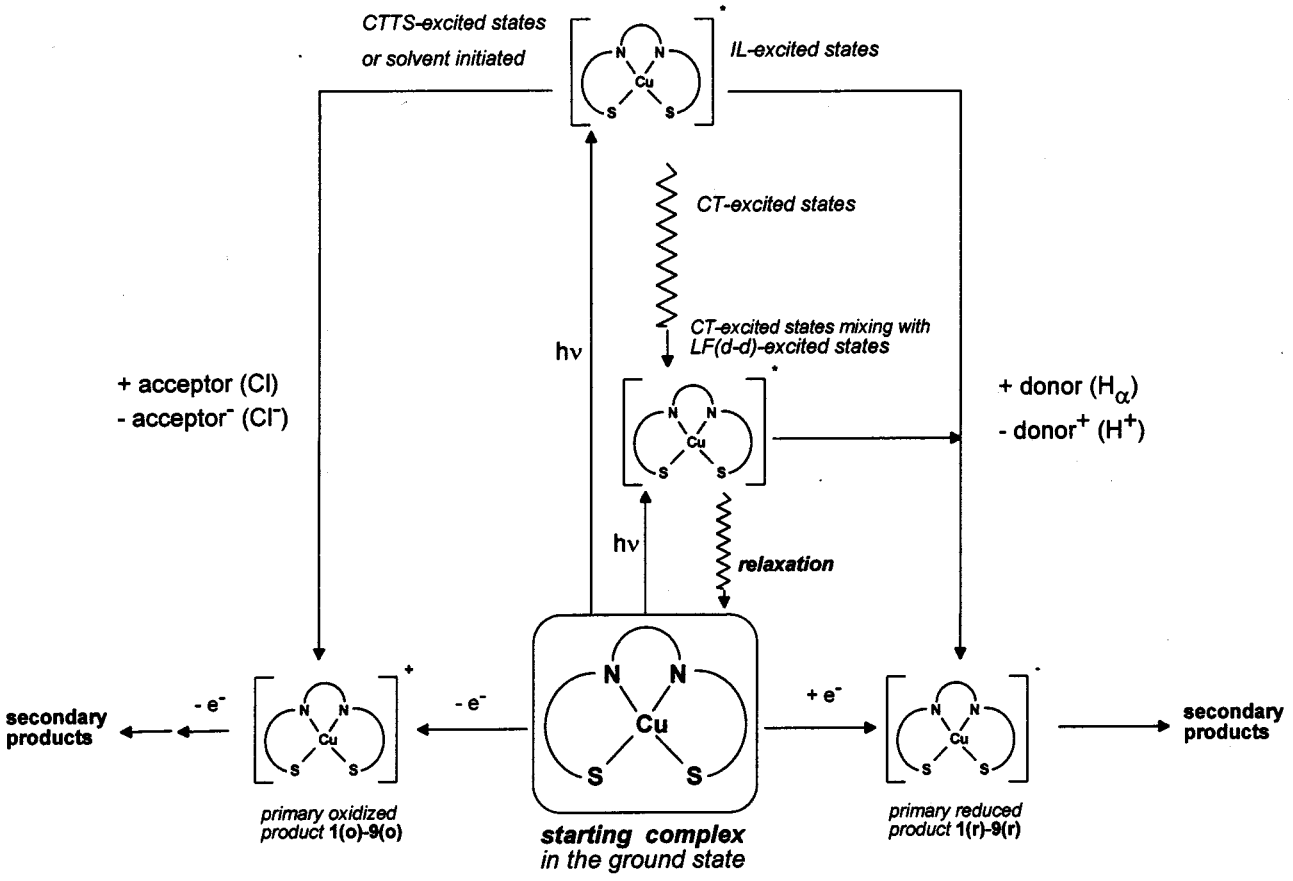

Scheme 1. General scheme of the electron-transfer pathway of the complexes **1**−**9**

Instrumentation

Spectroelectrochemistry: Cyclic voltammetry was performed in butyronitrile or THF using a standard vacuum-tight single-compartment cell equipped with a Pt disk working electrode of 0.42 mm^2 apparent surface area polished carefully with a 0.25 μm diamond paste. Pt gauze auxiliary and coiled Ag wire pseudoreference electrodes were used. The redox potentials are reported versus the $E_{1/2}$ potential of the ferrocene/ferrocenium (Fc/Fc^+) couple used as the recommended internal standard.[24] Occasionally, the cobaltocene/cobaltocenium ($CoCp_2^{+/0}$) couple was employed instead of Fc/Fc^+, using $E_{1/2}(CoCp_2^{+/0}) = -1.34$ V vs. Fc/Fc^+.[25] In butyronitrile $E_{1/2}(Fc/Fc^+) = +0.43$ V vs. SCE.[26] The cyclic voltammetric samples contained one of the $5\cdot10^{-4}$ M complexes **1**−**9** and $3\cdot10^{-1}$ M Bu_4NPF_6 as supporting electrolyte. UV/Vis spectroelectrochemistry at variable temperatures was carried out with previously described optically transparent thin-layer electrochemical (OTTLE) cells[27][28] placed into a Perkin-Elmer Lambda 5 spectrophotometer equipped with a 3600 data station. The solutions were typically $5\cdot10^{-3}$ M in the copper complexes **1**−**7** or less concentrated (near saturation) due to limited solubility of **8** and **9**, and $3\cdot10^{-1}$ M in the supporting electrolyte. Potential control during spectroelectrochemical experiments was achieved with a PA4 potentiostat (*EKOM*, Czech Republic).

Photochemistry: The photochemical experiments were carried out in 1-cm quartz cuvettes. The solutions typically contained ca. $5\cdot10^{-5}$ M **1**-**9**. As light source served a high-pressure mercury lamp USH 102DH (Ushio) equipped with appropriate filters or a monochromator (AMKO). Electronic absorption spectra were recorded in the course of the photochemical experiments with Cary 3 (Varian) and Perkin-Elmer Lambda 900 spectrophotometers.

Time-Resolved Spectroscopy: The third or fourth harmonic outputs (355 or 266 nm) of an Nd-Yag laser (GCR-11, Quanta-ray) were used for photoexcitation and a Xenon lamp (XBO 500, Narva) for probing the transient absorption in the ns and μs experiments. The light source for the ms experiments were two high-pressure mercury flash lamps operating parallel (Narva). The absorption was probed with an HBO 500 lamp (Narva). After each pulse, the sample solutions were replaced to avoid accumulation of photoproducts.

Acknowledgments

Financial support by the Deutsche Forschungsgemeinschaft, the Netherlands Foundation for Chemical Research (SON) and the Netherlands Organization for Pure Research (NWO) is gratefully acknowledged. We wish to thank Prof. O. Brede and his group (University of Leipzig) for the ns and μs time-resolved spectroscopic experiments.

[1] H. Hennig, S. Knoblauch, D. Scholz, *New J. Chem*. **1997**, *21*, 701−708; H. Hennig, M. Ecke, S. Knoblauch, *J. Inf. Rec.* **1996**, *23*, 131−134.
[2] L. Hennig, G. Mann, *Z. Chem*. **1988**, *28*, 364−365.
[3] H. Toftlund, J. Becher, P. H. Olesen, J. Z. Pedersen, *Isr. J. Chem*. **1985**, *21*, 56−65.
[4] L. Hennig, R. Kirmse, O. Hammerich, S. Larsen, H. Frydendahl, H. Toftlund, J. Becher, *Inorg. Chim. Acta* **1995**, *234*, 67−74.
[5] S. Mandal, G. Das, R. Singh, R. Shukla, P. K. Bharadwaj, *Coord. Chem. Rev.* **1997**, *160*, 191−235.
[6] J. Hanss, H.-J. Krüger, *Angew. Chem*. **1996**, *108*, 2989−2991; *Angew. Chem. Int. Ed. Engl.* **1996**, *35*, 2827−2830.
[7] G. Ferraudi, S. Muralidharan, *Coord. Chem. Rev.* **1981**, *36*, 45−88.
[8] O. Horváth, K. L. Stevenson, *Charge transfer photochemistry of coordination compounds*, VCH Publishers, New York, **1993**, chapter 4.1., p. 35−62.
[9] B. G. Jeliazkova, J. K. Panajotova, *Z. Naturforsch., B: Chem. Sci.* **1995**, *50*, 524−528.
[10] P. L. Verheijdt, J. G. Haasnoot, J. Reedijk, *Inorg. Chim. Acta* **1983**, *76*, L43−L46.
[11] B. G. Jeliazkova, N. D. Yordanov, *Inorg. Chim. Acta* **1993**, *203*, 201−204.
[12] B. G. Jeliazkova, M. A. Doicheva, *Polyhedron* **1996**, *15*, 1277−1282.
[13] B. G. Jeliazkova, G. C. Sarova, *J. Photochem. Photobiol. A* **1996**, *97*, 5−9.
[14] B. G. Jeliazkova, G. C. Sarova, *Polyhedron* **1997**, *16*, 3967−3975.
[15] D. M. Dooley, B. M. Patterson, *Inorg. Chem*. **1982**, *21*, 4330−4332.
[16] A. Vogler, H. Kunkely, *Inorg. Chem*.**1982**, 21, 1172−1175.
[17] A. Vogler, H. Kunkely, *J. Am. Chem. Soc.* **1981**, *103*, 1559−1560.
[18] A. Vogler, H. Kunkely, *Angew. Chem*. **1981**, *93*, 399−400; *Angew. Chem. Int. Ed. Engl.* **1981**, *20*, 386−387.
[19] R. Henning, W. Schlamann, H. Kisch, *Angew. Chem*. **1980**, *92*, 664−665; *Angew. Chem. Int. Ed. Engl*. **1980**, *19*, 645−646.
[20] W. Dietzsch, P. Strauch, E. Hoyer, *Coord. Chem. Rev.* **1992**, *121*, 43−130.
[21] T. Imamura, M. Ryan, G. Gordon, D. Coucouvanis, *J. Am. Chem. Soc.* **1984**, *106*, 984−990.
[22] H. Hennig, S. Knoblauch, R. Benedix, J. Sieler, S. Jelonek, F. Somoza, publication in preparation
[23] D. W. Hendrickson, Y. S. Sohn, H. B. Gray, *Inorg. Chem*. **1971**, *10*, 1559−1563.
[24] R. R. Gagné, C. A. Koval, G. C. Lisensky, *Inorg. Chem*. **1980**, *19*, 2854−2855.
[25] R. S. Stojanovic, A. M. Bond, *Anal. Chem*. **1993**, *65*, 56−64.
[26] B. D. Rossenaar, F. Hartl, D. J. Stufkens, C. Amatore, E. Maisonhaute, J. N. Verpeaux, *Organometallics* **1997**, *16*, 4675−4685.
[27] M. Krejcík, M. Danek, F. Hartl, *J. Electroanal. Chem., Interfacial Electrochem*. **1991**, *317*, 179−187.
[28] F. Hartl, H. Luyten, H. A. Nieuwhuis, G. Schoemaker, *Appl. Spectrosc.* **1994**, *48*, 1522−1528.
[29] T. Yamabe, K. Hori, T. Minato, K. Fukui, Y. Sugiura, *Inorg. Chem*. **1982**, *21*, 2040−2046.
[30] R. L. Harlow, W. J. Wells III, G. W. Watt, S. H. Simonsen, *Inorg. Chem*. **1975**, *14*, 1768−1773.
[31] P. K. Bharadwaj, J. A. Potenza, H. J. Schugar, *J. Am. Chem. Soc.* **1986**, *108*, 1351−1352.
[32] M. Gulliotti, L. Casella, A.Pintar, E. Suardi, P. Zanello, S. Mangani, *J. Chem. Soc., Dalton Trans.* **1989**, 1979−1986.
[33] R. D. Bereman, G. D. Shields, J. Bordner, J. Dorfman, *Inorg. Chem*. **1981**, *20*, 2165−2169.
[34] J. C. Rasmussen, H. Toftlund, A. N. Nivorizhkin, J. Bourassa, P. C. Ford, *Inorg. Chim. Acta* **1996**, *251*, 291−298.
[35] In contrast to our electrochemical findings, L. Hennig et al. found the reduction potential of **8** at a mercury film electrode in acetonitrile to be more negative by 0.33 V and 0.43 V than those of more planar **5** and **6**, respectively[4].
[36] S. Knoblauch, F. Somoza, unpublished results.
[37] H. J. Schugar, *Copper Coordination Chemistry: Biochemical and Inorganic Perspectives* (Eds.: K. D. Karlin, J. Zubieta), Adenine Press, New York, **1983**, p. 43−74.
[38] P. E. Hoggard, *Coord. Chem. Rev.* **1997**, *159*, 235−243.

Received July 9, 1998
[I98221]